

Experimental Biology and Medicine

Osteogenic activity of silymarin through enhancement of alkaline phosphatase and osteocalcin in osteoblasts and tibia-fractured mice

Jung-Lye Kim, Sin-Hye Park, Daewon Jeong, Ju-Suk Nam and Young-Hee Kang

Experimental Biology and Medicine 2012, 237:417-428.
doi: 10.1258/ebm.2011.011376 originally published online April 10, 2012

Updated information and services can be found at:
<http://ebm.rsmjournals.com/content/237/4/417>

This article cites 33 articles, 2 of which can be accessed free at:
<http://ebm.rsmjournals.com/content/237/4/417#BIBL>



© 2008 Society for Experimental Biology and Medicine

Osteogenic activity of silymarin through enhancement of alkaline phosphatase and osteocalcin in osteoblasts and tibia-fractured mice

Jung-Lye Kim¹, Sin-Hye Park¹, Daewon Jeong², Ju-Suk Nam³ and Young-Hee Kang¹

¹Department of Food and Nutrition, Hallym University, Chuncheon, Kangwon-do 200-702; ²Department of Microbiology, Laboratory of Metabolic Disease Control for Bone, College of Medicine, Yeungnam University, Daegu 705-717; ³Medical Science and Engineering Research Center, Hallym University, Chuncheon, Kangwon-do 200-702, Republic of Korea

Corresponding author: Prof Young-Hee Kang. Email: yhkang@hallym.ac.kr

Abstract

Bone-remodeling imbalance induced by increased bone resorption and osteoclast formation is known to cause skeletal diseases such as osteoporosis. There has been growing interest in the anabolic natural agents that enhance bone formation. Silymarin is flavonolignans extracted from blessed milk thistle. Several studies suggest that silymarin possesses antihepatotoxic properties and anticancer effects against carcinoma cells. This study investigated promoting effects of silymarin on differentiation and mineralization of osteoblastic MC3T3-E1 mouse cells and on bone mineral density (BMD) by *in vivo* fracture experiments. Osteoblasts were treated with 1–20 $\mu\text{mol/L}$ silymarin for 15 days in a differentiating medium. In addition, this study explored signaling pathways implicated in the osteoblastogenesis of silymarin. It was found that silymarin stimulated alkaline phosphatase (ALP) activity and calcium nodule formation in a dose-dependent manner with a substantial effect on osteoblast proliferation. Silymarin treatment enhanced collagen secretion, osteocalcin transcription and bone morphogenetic protein (BMP) expression. The BMP inhibitor noggin suppressed the silymarin-promoted ALP activity in differentiated osteoblasts, suggesting that its osteoblastogenic actions entail the BMP pathway. This was proved by increased SMAD1/5/8 phosphorylation and runt-related transcription factor 2 (Runx2) expression in the presence of silymarin. In 21-day fracture-healing experiments, fractured and silymarin (10 mg/kg)-treated C57BL/6 mice showed better bone healing than fractured mice. Silymarin supplementation improved tibial bone strength with elevated BMD and serum levels of osteogenic ALP and osteocalcin. Taken together, these results demonstrate, for the first time, that silymarin has a potential to enhance osteoblastogenesis through accelerating BMP/SMAD/Runx2 signal pathways and to improve fracture healing and bone strength in mouse tibiae.

Keywords: alkaline phosphatase, bone morphogenetic protein-2, osteocalcin, osteogenesis, silymarin, SMAD signaling

Experimental Biology and Medicine 2012; **237**: 417–428. DOI: 10.1258/ebm.2011.011376

Introduction

Bone homeostasis is maintained through balance between the bone resorption by osteoclasts and the bone formation by osteoblasts.¹ Bone formation is characterized by bone-specific extracellular matrix (ECM) protein expression and mineralization.² Bone matrix proteins synthesized by osteoblasts include collagen type I, alkaline phosphatase (ALP), osteopontin, bone sialoprotein and osteocalcin.³ These proteins are secreted to the ECM for mature bone matrix during bone formation. The accumulation of bone matrix protein in the ECM is known to be accompanied in parallel by matrix mineralization by calcium deposition.⁴ Expression of bone marker genes encoding bone matrix proteins takes

place in a well-coordinated temporal manner during bone formation. The bone formation requires three essential steps of osteoblast differentiation, matrix maturation and matrix mineralization.⁵

The transcription of the bone marker genes is regulated by a major bone-specific runt-related transcription factor 2 (Runx2).^{5,6} Runx2 influences osteogenesis by stimulating transcription of osteogenic target genes via binding its runt homology domain to target promoters and enhancers.^{6,7} Overexpression of Runx2 in osteoblastic MC3T3-E1 cells increases bone matrix mineralization, indicating that Runx2 plays an indirect stimulatory role in ECM mineralization.^{8,9} In addition, bone morphogenetic proteins (BMPs)

are involved in inducing osteoblastic differentiation.¹⁰ BMP initiates signaling by interacting with two distinct serine/threonine kinase receptors of type I and type II that can activate the cytoplasmic SMAD proteins in osteoblast differentiation.¹¹ BMP2 induces expression of Runx2 and osteocalcin as well as phosphorylation of Smad1/5/8. It has also been shown that constitutively active SMAD1 induces osteoblastic differentiation of C2C12 myoblasts in cooperation with SMAD4 or Runx2.¹²

Fracture repair of the bone is a complex process entailing the formation and resorption of ECM.¹³ The cartilaginous callus is formed at the fracture site and changed to new bone through the ossification process.¹⁴ During the fracture-healing process, damaged osteocytes and bone matrix are removed by phagocytes, followed by proliferation and differentiation of bone stem cells into osteoblasts that form the reparative matrix.¹⁵ The role of osteoblasts in the fracture repair process has thus been established.

Silymarin is a constitutive natural compound composed of an isomeric mixture of the flavonolignans of silychristin, isosilychristin, silydianin, silibinin and isosilibinin (Figure 1a).¹⁶ Silymarin is abundant in milk thistle (*Silybum marianum*) and has been clinically implicated in various liver diseases such as alcohol or drug intoxication and viral hepatitis, whose pathogenesis involves an inflammatory response.¹⁷ Information concerning modulation of bone marker genes by silymarin is very limited. Silymarin was found to be ineffective in proliferative activity and osteocalcin secretion in rat calvarial osteoblast-like cells.¹⁸ It has been reported that several natural compounds found in plant sources are promising in maintaining an optimal bone status and stimulating bone formation.^{12,18,19} Hesperidin, present in citrus fruits, may regulate osteoblast differentiation through BMP signaling, and influence the mineralization process by modulating

osteopontin expression.²⁰ Osthole, a coumarin derivative present in many medicinal plants, mediates cell differentiation through the BMP2/p38 and extracellular signal-regulated kinase 1/2 pathways in human osteoblast cells.²¹

There are very few published reports that definitely demonstrate the stimulatory effects of silymarin on osteoblast differentiation, gene transcription and ECM mineralization. In considering these major events for bone-forming osteogenesis, this study evaluated whether silymarin boosted bone marker protein expression and matrix mineralization in mouse origin osteoblastic MC3T3-E1 cells. In addition, this study used an *in vivo* mouse tibia fracture model to confirm the benefit of silymarin supplementation on fracture healing and bone regeneration. We report here, for the first time, that silymarin can be a direct regulator for osteoblast differentiation, bone anabolic formation and fracture healing.

Materials and methods

Materials

Fetal bovine serum (FBS), penicillin-streptomycin, trypsin-ethylenediaminetetraacetic acid were purchased from Lonza (Walkersville, MD, USA). 3-(4,5-Dimethylthiazol-yl)-diphenyl tetrazoliumbromide (MTT) was provided by Duchefa Biochemie (Haarlem, the Netherlands). Minimum essential medium alpha (α -MEM), silibinin and silymarin were purchased from Sigma-Aldrich Chemicals (St Louis, MO, USA), as were all other reagents, unless specifically stated as from elsewhere. Antibodies of mouse type I collagen and BMP-2 were purchased from Santa Cruz Biotechnology (Santa Cruz, CA, USA) and Abcam (Cambridge, UK), respectively. Antibodies of mouse phosphate SMAD1/5/8, and SMAD4 were purchased

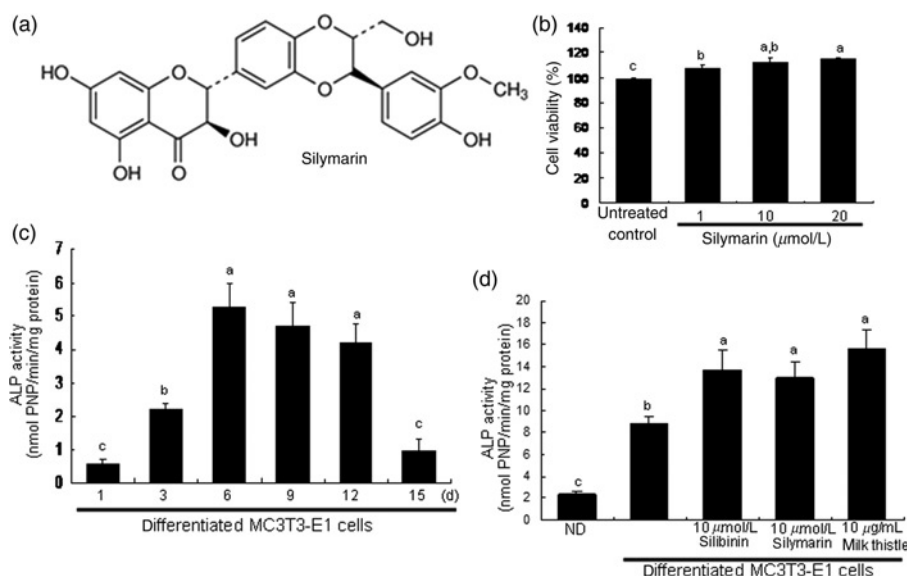


Figure 1 Chemical structure (a) and cytotoxicity (b) of silymarin, and alkaline phosphatase (ALP) secretion (c and d). Osteoblastic MC3T3-E1 cells were cultured for 15 days in the presence of 1–20 μ M/L of silymarin (b). Cell toxicity was measured by 3-(4,5-dimethylthiazol-yl)-diphenyl tetrazoliumbromide assay. Values are presented as mean \pm SEM ($n = 5$) and expressed as percent cell survival relative to untreated cells (cell viability = 100%). Time course responses of ALP secretion for 15 d (c) and its enhancement by silibinin, silymarin and milk thistle (d) were assessed in MC3T3-E1 cells differentiated for six days. Absorbance was measured at $\lambda = 405$ nm and compared with *p*-nitrophenol (PNP) standard. ALP enzyme activity in media was expressed as nmol PNP/min/mg protein (mean \pm SEM, $n = 4$). Values in bar graphs not sharing a letter indicate significant difference at $P < 0.05$.

from Cell Signaling Technology (Beverly, MA, USA). Horseradish peroxidase-conjugated goat anti-rabbit IgG, goat anti-mouse and donkey anti-goat IgG were provided by Jackson ImmunoResearch Laboratories (West Grove, PA, USA). Cyanine 3-conjugated goat anti-rabbit IgG was provided by Rockland (Gilbertsville, PA, USA). BMP inhibitor (noggin) was obtained from R&D systems (Minneapolis, MN, USA). Reverse transcriptase and Taq DNA polymerase were purchased from Promega (Madison, WI, USA). Silymarin and silybinin were dissolved in dimethyl sulfoxide for live culture with cells; its final culture concentration was <0.5%.

MC3T3-E1 cell culture and osteoblast differentiation

Osteoblastic MC3T3-E1 cells (mouse calvaria origin) were cultured at 37°C in a humidified atmosphere of 5% CO₂ in air. MC3T3-E1 cells were incubated in α -MEM containing 10% FBS, 2 mmol/L glutamine, 100 U/mL penicillin and 100 μ g/mL streptomycin. For the osteoblast differentiation,⁴ MC3T3-E1 cells were seeded on 24-well plates and grown to \approx 90% confluence, and then the culture medium was changed to a fresh osteogenic medium containing 10 mmol/L β -glycerolphosphate and 50 μ g/mL ascorbic acid to initiate matrix mineralization. Cell culture medium was changed every three days for 15 days.

Cell proliferation and toxicity were determined using a colorimetric assay based on the uptake of MTT by viable cells.²² After exposure to various concentrations of silymarin for 15 days, a solution of MTT (1 mg/mL) was added to cells and incubated at 37°C to allow cleavage of the tetrazolium ring by mitochondrial dehydrogenase, resulting in the formation of blue formazan crystals. After 3 h, the purple formazan product was dissolved in 0.5 mL of isopropanol with gentle shaking. Absorbance of formazan dye was measured at λ = 570 nm with background subtraction using λ = 690 nm. The viability of MC3T3-E1 cells was dose-dependently increased by 1–20 μ mol/L silymarin during 15-day differentiation (Figure 1b), suggesting that non-toxic silymarin stimulated osteoblast proliferation.

Measurement of ALP activity

ALP activity of MC3T3-E1 cells was measured by a modified colorimetric enzyme assay.²³ After culture protocols, cells were lysed with 0.2% Triton X-100 and the lysates were centrifuged at 14,000 \times g for 10 min at 4°C. Lysate aliquots were incubated with 0.5 mol/L Tris-HCl buffer (pH 9.9) containing 6 mmol/L of *p*-nitrophenyl phosphate and 1 mmol/L of MgCl₂ at 37°C for 1 h. The protein contents of lysates were determined by the Lowry method. ALP activity was expressed as nmol *p*-nitrophenol (PNP) produced/min/mg protein. Absorbance was measured at λ = 405 nm and compared with PNP standards.

ALP staining for matrix enzyme activity was also performed by using alkaline phosphatase kit (Sigma). After six-day culture protocols, cells were washed with phosphate buffered saline (PBS) and fixed with 4% formaldehyde, rinsed with deionized water, and stained under protection from direct light. ALP staining was carried out by adding for 30 min 0.1 mol/L of Tris buffer (pH 9.0) containing

0.6 mg/mL of Fast Blue RR salt and 0.2 mg/mL of naphthol As-Mx phosphate disodium salt as substrate for the cell layers.

Measurement of ECM calcium deposits

Staining with alizarin red S is used to visualize bone nodule formation and calcium deposition of osteoblasts. As the dye forms a complex with ECM calcium by chelation, heavy reddish staining of alizarin red S is proportional to the area of mineralized ECM.²⁴ At harvest, MC3T3-E1 cells were fixed with 70% ethanol for 1 h and stained with 40 mmol/L of alizarin red S (pH 4.2) for 10 min. To quantify bound dye, the stain was solubilized in 10 mmol/L of sodium phosphate buffer (pH 7.0) with 1 mL 10% (W/V) cetylpyridinium chloride. Absorbance of the solubilized stain was measured at λ = 562 nm by using a spectrophotometer.

Western blot analysis

Western blot analysis was carried out using culture medium and cell lysates prepared from cultured MC3T3-E1 cells. Equal volumes of culture media and equal amounts of lysate proteins were electrophoresed on 6–12% sodium dodecyl sulfate polyacrylamide gel electrophoresis and transferred onto a nitrocellulose membrane. Non-specific binding was blocked by soaking membranes in a Tris-buffered saline-Tween buffer (50 mmol/L Tris-HCl [pH 7.5], 150 mmol/L NaCl, and 0.1% Tween 20) containing 3% bovine serum albumin or 5% non-fat milk for 3 h. The membranes were incubated with polyclonal goat anti-mouse collagen type I, polyclonal rabbit anti-mouse BMP-2, polyclonal rabbit anti-mouse SMAD1/5/8 or polyclonal rabbit anti-mouse SMAD4. The membranes were then incubated with a secondary antibody, a goat anti-rabbit IgG, goat anti-mouse IgG or donkey anti-goat IgG conjugated to horseradish peroxidase. The protein levels on gels were determined by using Supersignal West Pico Chemiluminescence detection reagents (Pierce Biotechnology, Rockford, IL, USA) and Konica X-ray film (Konica, Tokyo, Japan). Incubation with monoclonal mouse β -actin antibody was conducted for a comparative control.

Realtime reverse transcriptase polymerase chain reaction analysis

Following differentiation protocols, total RNA was isolated from MC3T3-E1 osteoblasts using a commercially available Trizol reagent kit (Invitrogen, Carlsbad, CA, USA). The isolated RNA (5 μ g) was reversibly transcribed with 200 units of reverse transcriptase and 0.5 μ g of oligo-(dT)¹⁵ primer (Bioneer Co, Daejeon, Korea). The expression of mRNA transcripts of osteocalcin (forward primer: 5' GAGGACAGGGA GGATCAAGT 3', reverse primer: 5' TGCTTGTGACGACT CTATCAG 3'), Runx2 (forward primer: 5' AAGTGCGGT GCAAACCTTCT 3', reverse primer: 5' TCTCGGTGGCTGGT AGTGA 3') and glyceraldehyde-3-phosphate dehydrogenase (GAPDH; forward primer: 5' TTGTCAAGCTCATTTTCCT GGTATG 3', reverse primer: 5' GCCATGTAGGCCAT

GAGGTC 3') were quantified by realtime reverse transcriptase polymerase chain reaction (RT-PCR) using a SYBR Green PCR kit (Qiagen, Valencia, CA, USA). Data analysis of realtime RT-PCR results and calculation of the relative quantitations were performed using Delta CT analysis by the Rotor-Gene software, version 6.0 (Corbett Research, Mortlake, Australia). The housekeeping gene GAPDH was used for internal normalization. The standard PCR conditions were 95°C for 10 min, then 40 cycles at 95°C (15 s), 60°C (15 s) and 72°C (20 s), followed by melting curve analysis.

Immunocytochemical analysis

MC3T3-E1 cells grown on glass slides were washed with PBS containing 0.2% Tween 20 (PBS-T), fixed with 4% ice-cold formaldehyde for 20 min and made permeable with 0.1% Triton X-100 and 0.1% sodium citrate for 2 min on ice. For blocking any non-specific binding, cells were incubated for 1 h with 20% FBS in PBS-T. After being washed, fixed cells were incubated overnight with polyclonal anti-mouse phosphorylated SMAD1/5/8 and SMAD4 in PBS-T at 4°C. Fluorescein isothiocyanate-conjugated anti-rabbit IgG or cyanine 3-conjugated anti-rabbit IgG in PBS-T was added as a secondary antibody. Fluorescent images were taken with an Axioimager Optical fluorescence microscope (Zeiss, Oberkochen, Germany).

Animals

To determine *in vivo* effects of silymarin on fracture healing and bone regeneration, this study used mouse fracture models. C57BL/6J mice (4 weeks of age, 25–30 g) were obtained from the Experimental Animal Center, Hallym University, and kept on a 12 h light/12 h dark cycle at 20–25°C with 60% relative humidity under specific pathogen-free conditions. Mice were fed a standard rodent chow diet (CJ Feed, Seoul, Korea) during the experimental period (14–21 days) with free access to water *ad libitum* at the animal facility of Hallym University. The animals were allowed to acclimatize for a week before beginning the experiments. All animal experiments were performed in accordance with the University's Guidelines for the Care and Use of Laboratory Animals approved by the Committee on Animal Experimentation of Hallym University (permission number: hallym 2010–75).

Tibial fracture and silymarin treatments

A technique for standardized experimental fracture in the mouse tibiae was adapted for mouse fracture repair models.^{25,26} Mice were randomly divided into three experimental groups with six mice in each group: unfractured controls without fracture and receiving surgical implants, animals tibially fractured and receiving surgical implants, and animals tibially fractured and receiving surgical implants followed by oral treatment with 10 mg/kg per body weight (BW) silymarin once a day for 14–21 days. The mice were anesthetized with an intraperitoneal injection of Zoletil (40 mg/kg BW) mixed with Rompun (10 mg/kg BW). Unfractured controls and fractured animals received the

vehicle saline for 14–21 days after fracture. Tibiae were fractured by an impact device and absorbable sutures were used to close the intramuscular septum and skin incision. To achieve stable tibial fixation, a 0.2 mm sterilized stainless-steel pin was implanted into the intramedullary canal, beginning in the knee between the tibial condyles and exiting the greater trochanter of the tibia. The pin was cut as close as possible to the knee articular cartilage and driven proximally so that the tip was flush with the cartilage.

Bone analysis and measurement of bone formation markers

For the analysis of *in vivo* fracture healing, the mouse tibiae were scanned using a microcomputer tomography (CT) scanner (MicroCAT II scanner; Siemens Preclinical Solutions, Knoxville, TN, USA). Three-dimensional images were reconstructed using the reconstruction utility and visualized for the bone analysis. The bone mineral density (BMD) and bone mineral content (BMC) of the mouse tibial bone were determined with a PIXImus mouse densitometer (GE Lunar; GE Healthcare, Waukesha, WI, USA) under anesthesia to monitor the initial pin fixation as well as ongoing callus formation. BMD was calculated by dividing BMC (mg) by the projected bone area (cm²) and assessed in the region of the callus on days 1, 7 and 14 after the fracture episode.

All serum samples obtained by centrifugation (3000 rpm for 10 min) were stored at –70°C prior to analysis. Serum levels of osteocalcin were measured by using osteocalcin enzyme-linked immunosorbent assay (ELISA) kits (Uscn Life Science, Wuhan, China) according to the manufacturer's instructions. Serum ALP activity was determined by incubating 6 mmol/L of *p*-nitrophenyl phosphate as the substrate in 0.5 mol/L of Tris–HCl buffer (pH 9.9) containing 1 mmol/L of MgCl₂ at 37°C for 30 min and by measuring absorbance at $\lambda = 405$ nm. A unit of ALP activity was defined as release of 1 μ mol of PNP/min.

Statistical analyses

The data are presented as mean \pm SEM. Statistical analyses were carried out using Statistical Analysis Systems statistical software package (SAS Institute Inc, Cary, NC, USA). Significance was determined by one-way analysis of variance, followed by the Duncan range test for multiple comparisons. Differences were considered significant at $P < 0.05$.

Results

Effects of silymarin on ALP secretion

ALP secretion is an early- and mid-stage biomarker for matrix maturation of osteoblasts. The ALP activity, expressed as PNP production/min/mg cell protein, peaked at the proliferation stage on day 6 during the 15-day differentiation of MC3T3-E1 cells (Figure 1c). The ALP secretion was markedly enhanced in six-day differentiated cells treated with 10 μ mol/L of silibinin, 10 μ mol/L of silymarin or 10 μ g/mL of milk thistle.

The colorimetric enzyme assay revealed that treatment with 1–20 $\mu\text{mol/L}$ of silymarin dose-dependently elevated ALP activity at the six-day proliferation stage of MC3T3-E1 cells cultured in normal osteogenic medium (Figure 2a). From ALP staining for matrix enzyme activity, there was a weak staining for the basal ALP activity in undifferentiated MC3T3-E1 cells, where heavy lilac staining was observed in differentiated cells, indicative of increased ALP secretion into the ECM (Figure 2b). Addition of 1–20 $\mu\text{mol/L}$ of silymarin considerably promoted the staining levels of ALP in a dose-dependent manner.

Mineralization and deposition of ECM by silymarin

With alizarin red S staining, ECM calcium deposits revealed as reddish-brown staining were barely detected at seven-day differentiation (Figure 3a). However, on day 15, there was a heavy staining of alizarin red S, indicating that bone nodules formed by calcium deposits were notably enhanced. Addition of silymarin to MC3T3-E1 cells in osteogenic medium augmented calcium deposits in a dose-dependent manner (Figure 4b). This was consistent with a dose-dependent increase in colorimetric staining intensity by treating with 1–20 $\mu\text{mol/L}$ of silymarin (Figure 4b, bottom panel).

Silymarin modulation of collagen I and osteocalcin production

Collagen I is a major extracellular collagenous protein for organic matrix formation in bone.²⁴ As expected, collagen I secretion attained the peak on days 3–6 and gradually

subsided afterward until day 15 (Figure 4a), indicative of being an early-mid-stage biomarker. The presence of silymarin dose-dependently increased collagen I secretion on day 6, suggesting that silymarin can promote ECM accumulation (Figure 4b). Therefore, collagen I secretion was boosted in a similar manner to ALP secretion.

This study attempted to examine modulation of osteocalcin, a bone marker gene, by silymarin. Transcriptional expression of osteocalcin (late osteoblast differentiation) was maximally increased on day 9 (Figure 4c), and was further enhanced in the presence of $\geq 10 \mu\text{mol/L}$ of silymarin (Figure 4d).

Elevation of BMP-2 level by silymarin

Protein expression of BMP, another osteoblast differentiation marker, was markedly increased at the very early stage of differentiation on day 1 in MC3T3-E1 cells cultured in osteogenic medium and sustained until day 9 (Figure 5a). BMP-2 induction was further enhanced in $\geq 10 \mu\text{mol/L}$ silymarin-treated osteoblasts cultured in osteogenic medium (Figure 5b).

Differentiation-elevated ALP secretion was mitigated below its basal level in the presence of 100 ng/mL of noggin, a BMP receptor inhibitor (Figure 5c). Accordingly, it was proved that ALP secretion entailed induction of membrane protein BMP-2. When osteoblasts were supplemented with 1–20 $\mu\text{mol/L}$ of silymarin in osteogenic medium, the noggin-abolished ALP secretion was restored back to the basal level. It should be noted that silymarin may boost ALP secretion independent of BMP-2 induction.

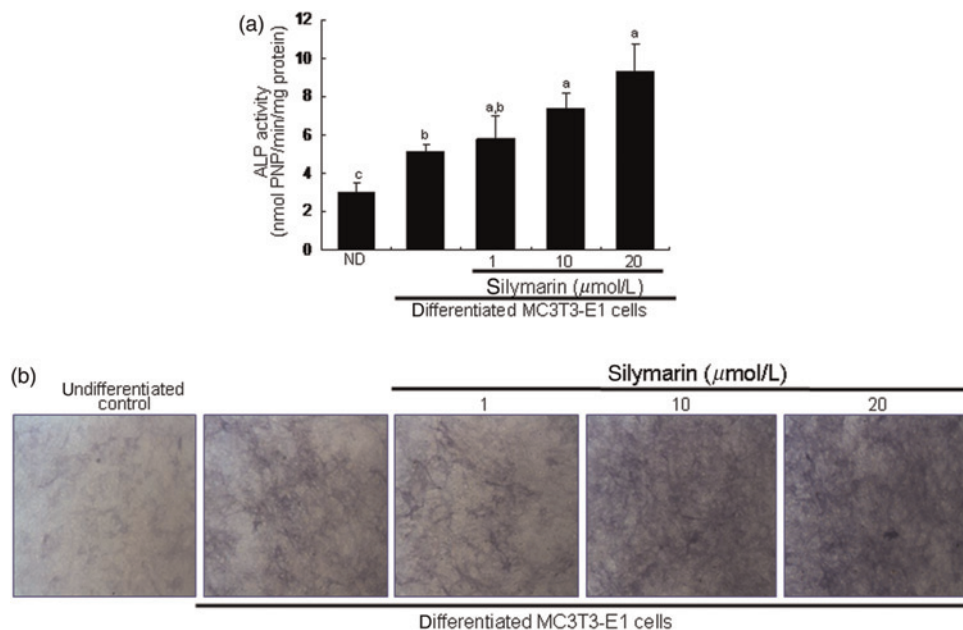


Figure 2 Upregulation of alkaline phosphatase (ALP) secretion by silymarin. To detect activity of ALP enzyme in media, a colorimetric enzyme assay was used (a). Increasing effects of 1–20 $\mu\text{mol/L}$ silymarin on ALP activity were examined in MC3T3-E1 cells on day 6. Absorbance was measured at $\lambda = 405 \text{ nm}$ and compared with *p*-nitrophenol (PNP) standard (mean \pm SEM, $n = 4$). The ALP enzyme activity was expressed as nmol PNP/min/mg protein. Values in bar graphs not sharing a letter indicate significant difference at $P < 0.05$. In another set of staining experiments (b), MC3T3-E1 cells were cultured on glass chamber plates for six days in the presence of 1–20 $\mu\text{mol/L}$ silymarin. Lilac staining intensity was proportional to the content of ALP secreted from MC3T3-E1 cells. Microphotographs were taken after an addition of naphthol As-Mx phosphate disodium salt to cell layers. (A color version of this figure is available in the online journal)

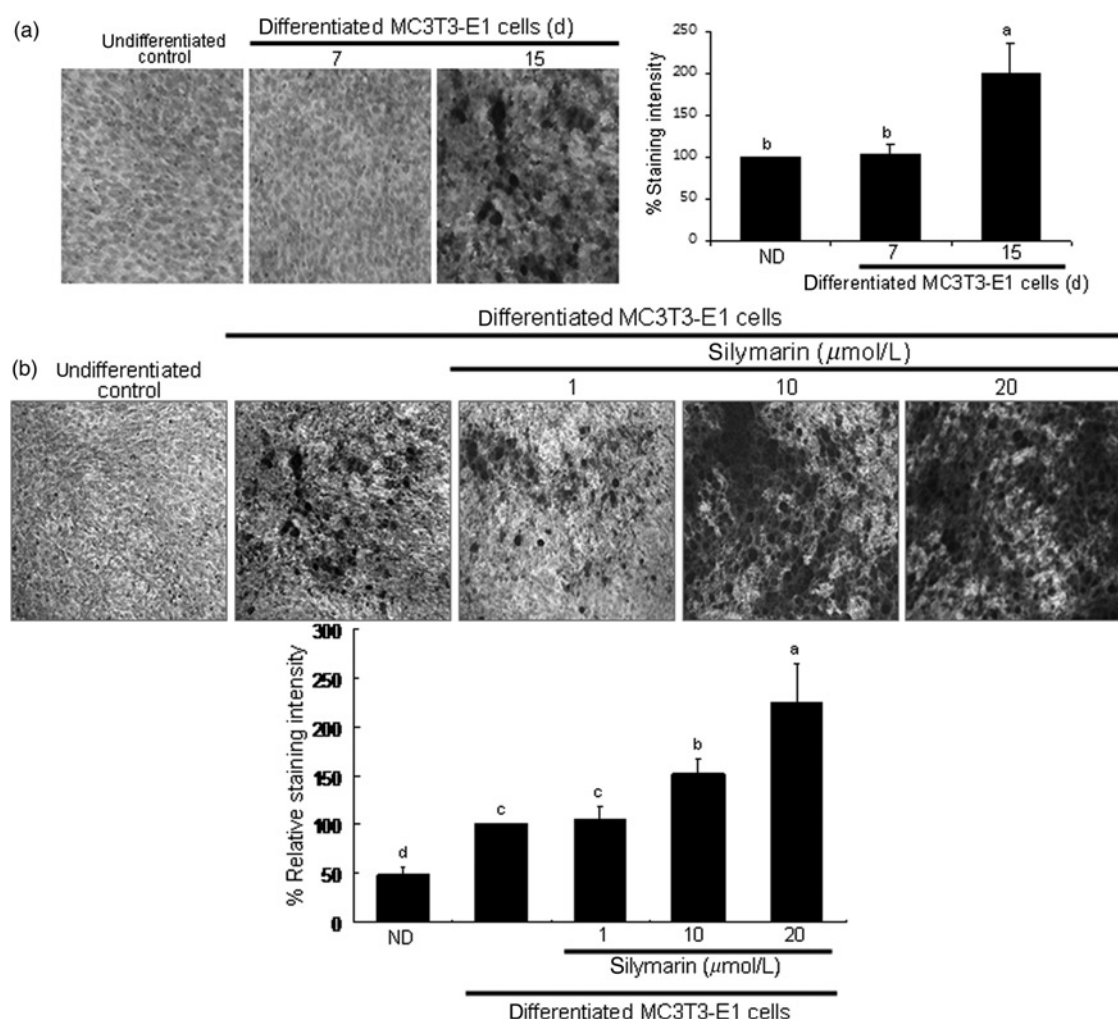


Figure 3 Enhancement of matrix mineralization in MC3T3-E1 cells by silymarin. Extracellular matrix (ECM) calcium deposits (bone nodule formation) for matrix mineralization were measured by alizarin red S staining. Cells were cultured in 24-well plates for 7 and 15 days (a). In another set of experiments, MC3T3-E1 osteoblasts were cultured in 24-well plates for 15 days in the presence of 1–20 $\mu\text{mol/L}$ of silymarin (b). Heavy reddish staining of alizarin red S was proportional to the area of mineralized ECM. Quantification for the intensity of alizarin red S staining was spectrophotometrically conducted at $\lambda = 562 \text{ nm}$. The bar graphs (mean \pm SEM, $n = 5$) represent quantitative results obtained from the spectrophotometer. Values not sharing a letter indicate significant difference at $P < 0.05$.

Stimulation of SMAD signaling and Runx2 transcription by silymarin

Binding of BMP to its receptor complex results in the activation of BMPRI, which in turn phosphorylates SMAD1/5/8 molecules, forming a complex with SMAD4 that translocates into the nucleus to activate transcription of specific genes.^{10,11}

When MC3T3-E1 cells were cultured in osteogenic medium, SMAD1/5/8 phosphorylation rapidly increased within 30 min and diminished after 60 min (Figure 6a). As shown in Figure 6b, stimulation of osteoblasts with 1–20 $\mu\text{mol/L}$ of silymarin boosted SMAD1/5/8 phosphorylation in a dose-dependent manner. In addition, the immunocytochemical analysis confirmed the boosting effects of silymarin on SMAD1/5/8 activation. There was relatively weak activation of SMAD1/5/8 in undifferentiated cells. Heavy nuclear staining in differentiated cells was observed, indicating that more SMAD1/5/8 was activated and translocated into the nucleus (Figure 6c). In cells treated with silymarin, fluorescent staining of nuclear SMAD1/5/8 was further enhanced.

Western blot analysis revealed that SMAD4 induction was also enhanced in a similar manner to SMAD1/5/8 activation in cells treated with silymarin in osteogenic medium (Figure 6b). Consistently, immunocytochemical staining proved that silymarin dose-dependently intensified the nuclear staining of SMAD4 (Figure 6c).

The expression of these bone marker genes is modulated by bone-specific transcription factor Runx2.²⁷ Runx2 transcription was increased on day 3 and thereafter diminished back to basal level (Figure 7a). Realtime PCR assay found that treatment of three-day differentiated cells with $\geq 10 \mu\text{mol/L}$ of silymarin promoted Runx2 transcription (Figure 7b). Accordingly, secretion of collagen I, ALP and osteocalcin was enhanced through eliciting Runx2 transcription.

Effects of silymarin on fracture healing

On day 21, microCT radiographic images of silymarin-treated mice showed notably better bone healing and remodeling of the tibial fracture compared with fractured mice (Figure 8). The morphology of tibial bones of silymarin-treated mice

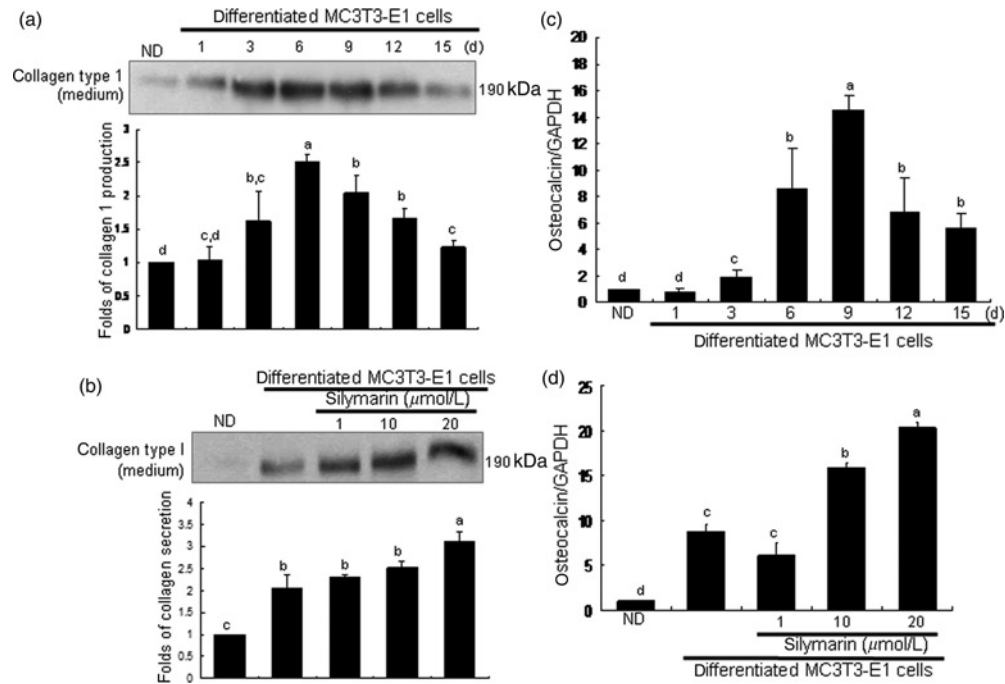


Figure 4 Elevation of collagen type I secretion and transcriptional expression of osteocalcin. Collagen I secretion was assessed in culture media collected from MC3T3-E1 cells differentiated for 15 days (a). In addition, MC3T3-E1 cells were cultured for 6 days in the presence of 1–20 $\mu\text{mol/L}$ of silymarin (b). Collagen I secretion in media was examined by Western blot analysis with a primary antibody against collagen I. The bar graphs (mean \pm SEM, $n = 3$) in the bottom panels represent quantitative results obtained from a densitometer. Time course response of expression of osteocalcin was evaluated in MC3T3-E1 cells for 15 days (c). In addition, mRNA expression of osteocalcin was examined in MC3T3-E1 cells incubated in the presence of 1–20 $\mu\text{mol/L}$ of silymarin (d). After culture protocols, realtime polymerase chain reaction analysis was carried out for the measurements of osteocalcin mRNA levels (mean \pm SEM, $n = 3$). The housekeeping gene glyceraldehyde-3-phosphate dehydrogenase (GAPDH) was used for internal normalization. Values in bar graphs not sharing a letter are different at $P < 0.05$

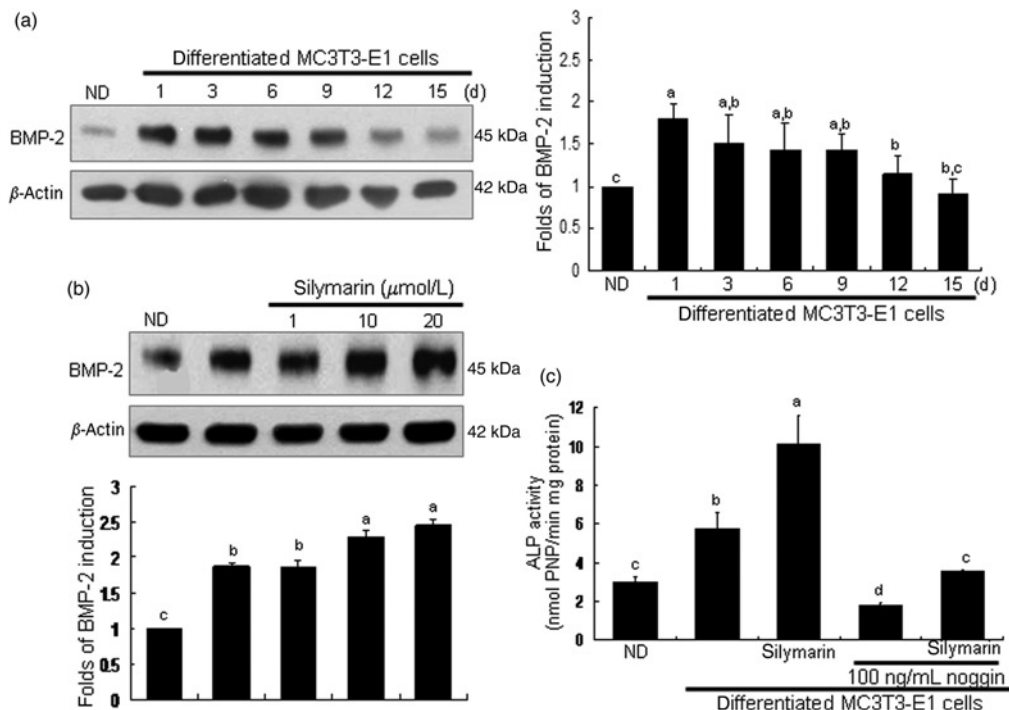


Figure 5 Elevation of bone morphogenetic protein (BMP)-2 by silymarin and noggin-suppressed alkaline phosphatase (ALP) activity in MC3T3-E1 cells. Time course response of BMP-2 induction was determined in MC3T3-E1 cells differentiated for 15 days (a). In addition, MC3T3-E1 cells were cultured for 1 day in the presence of 1–20 $\mu\text{mol/L}$ of silymarin (b). Cell lysates were subjected to Western blot analysis with a primary antibody against BMP-2. Representative blot data were respectively obtained from three independent experiments and β -actin protein was used as an internal control. The bar graphs (mean \pm SEM, $n = 3$) represent quantitative results obtained from a densitometer. The ALP secretion in media was examined on day 6 in MC3T3-E1 cells treated with 20 $\mu\text{mol/L}$ of silymarin in the presence of 100 ng/mL of noggin, the BMP antagonist (c). ALP activity was measured by a colorimetric enzyme assay and expressed as nmol PNP/min/mg protein ($n = 3$). Values not sharing a letter are different at $P < 0.05$

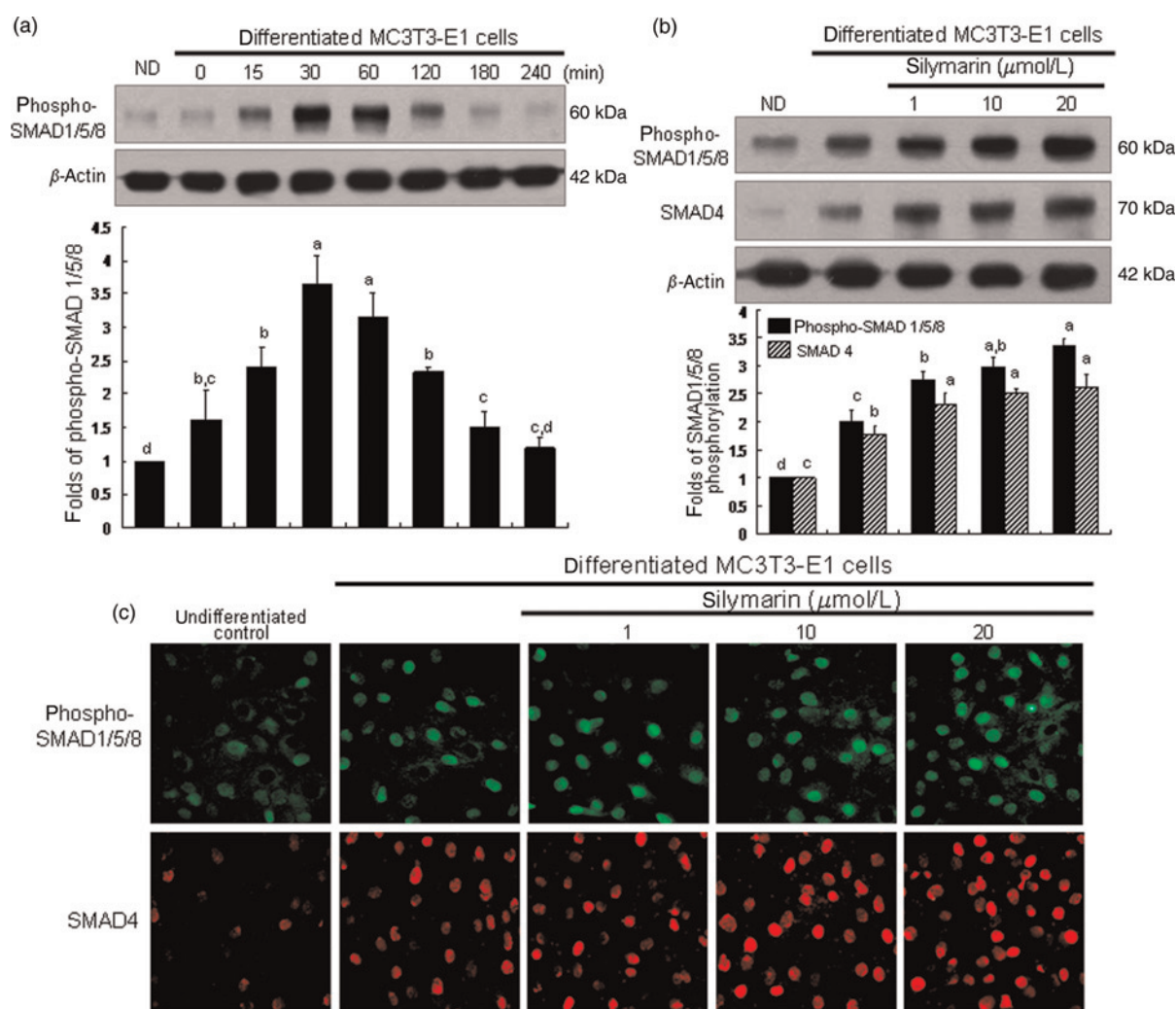


Figure 6 Further activation of SMAD1/5/8 and SMAD4 in osteoblastic MC3T3-E1 cells treated with silymarin. Time course response of SMAD1/5/8 phosphorylation was evaluated in MC3T3-E1 cells for 240 min (a). Activation of SMAD1/5/8 and SMAD4 was examined in MC3T3-E1 cells cultured for 30 min in the presence of 1–20 $\mu\text{mol/L}$ of silymarin (b). After culture protocols, cell lysates were subject to sodium dodecyl sulfate polyacrylamide gel electrophoresis and Western blot analysis with a primary antibody against phosphorylated SMAD1/5/8 or SMAD4. Representative blot data were respectively obtained from three independent experiments, and β -actin protein was used as an internal control. The bar graphs (mean \pm SEM, $n = 3$) in the bottom panels represent quantitative results obtained from a densitometer. Values not sharing a letter are different at $P < 0.05$. In addition, immunocytochemical analysis was conducted to measure nuclear translocation of SMAD1/5/8 and SMAD4 (c). After culture protocols, fixed cells were incubated with a primary antibody against phosphorylated SMAD1/5/8 or SMAD4. Fluorescein-conjugated anti-rabbit IgG (phosphorylated SMAD1/5/8) and cyanine 3-conjugated anti-rabbit IgG (phosphorylated SMAD4) were added as the secondary antibody. Fluorescent images were taken with a fluorescence microscope

was comparable to, if not indistinguishable from, that of unfractured controls.

The results for BMD measurements are summarized in Table 1. The BMD and BMC were markedly elevated in silymarin-treated animals during the 14-day healing period. These values were significantly higher than those of fractured mice from one week after the fracture, demonstrating that the supplementation of silymarin improved tibial bone strength. However, it should be noted that the BMC was greatly enhanced in fractured mice for healing.

One day after fracture surgery, the serum ALP levels declined up to $\approx 60\%$ even in unfractured controls, most likely due to surgery trauma (Table 2). The serum ALP level of silymarin-treated mice was restored on day 14 after fracture, unlike those of unfractured controls and fractured mice. The fracture surgery minimally influenced the

serum levels of another bone marker, osteocalcin, in fractured mice (Table 2). However, the osteocalcin levels were elevated in silymarin-treated mice during the fracture healing of 14 days. Consistent with osteoblast culture data (Figures 4c and d), silymarin was an osteogenic compound boosting levels of osteocalcin responsible for late osteoblast differentiation.

Discussion

Bone formation requires the three essential steps of osteoblast differentiation, matrix maturation and matrix mineralization.⁵ Bone formation of osteoblasts is characterized by cellular expression and synthesis of bone marker gene proteins for matrix maturation and by ECM mineralization triggered by calcium deposition.² Expression of bone marker

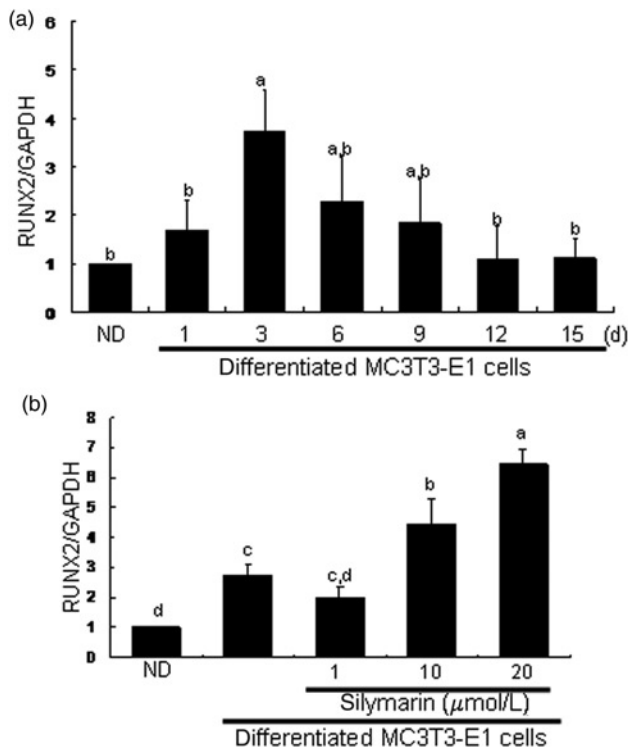


Figure 7 Transcriptional expression of runt-related transcription factor 2 (Runx2) in osteoblastic MC3T3-E1 cells treated with silymarin. Time course response of Runx2 transcription was evaluated in MC3T3-E1 cells for 15 days (a). In addition, mRNA expression of Runx2 was examined in MC3T3-E1 cells incubated in the presence of 1–20 $\mu\text{mol/L}$ of silymarin (b). After culture protocols, realtime polymerase chain reaction analysis was carried out for the measurement of Runx2 (on day 3) mRNA levels (mean \pm SEM, $n = 3$). The housekeeping gene glyceraldehyde-3-phosphate dehydrogenase (GAPDH) was used for internal normalization. Values in bar graphs not sharing a letter are different at $P < 0.05$

genes for osteoblast differentiation occurs during bone formation in a well-coordinated temporal manner. Bone matrix proteins synthesized by osteoblasts include collagen type I, ALP, osteopontin, bone sialoprotein and osteocalcin.³ The accumulation of bone matrix proteins in the ECM is accompanied by matrix mineralization.⁴

There are very few published reports that definitely display the stimulatory effects of silymarin on osteoblast differentiation, bone marker gene transcription and ECM mineralization. In this study, using the osteoblastic MC3T3-E1 cells, we investigated the influence of silymarin on osteoblast differentiation, ECM calcium deposits for matrix mineralization and protein expression and transcription of ECM bone-specific proteins. In addition, *in vivo* mouse fracture models were used to determine the improving effects of silymarin on fracture healing and bone strength. This study demonstrated that, at the stage of osteoblast differentiation, protein expression of ALP and collagen I, and transcription of osteocalcin were further enhanced by silymarin in a well-organized temporal manner. It was also found that silymarin supplementation distinctly improved bone healing and remodeling of the tibial fracture and increased serum levels of the bone marker proteins of ALP and osteocalcin.

Silymarin is a natural compound composed of an isomeric mixture of the flavonolignans of silychristin,

isosilychristin, silydianin, silibinin and isosilibinin.¹⁶ Silymarin is abundant in milk thistle and has been clinically implicated in liver diseases and viral hepatitis, whose pathogenesis involves an inflammatory response.¹⁷ Information on silymarin influencing bone marker genes is very limited. Silymarin was not effective in proliferative activity and osteocalcin secretion in rat calvarial osteoblast-like cells.¹⁸ However, some plant compounds have been shown to maintain an optimal bone status and stimulate bone formation.^{12,19,20} The glycoside hesperidin, found rich in citrus fruits, regulated osteoblast differentiation and maneuvered the mineralization process associated with osteopontin expression.²⁰ In addition, osthole, a coumarin derivative present in many medicinal plants, mediated cell differentiation through the BMP-2/p38 and extracellular signal-regulated kinase 1/2 pathways in human osteoblast cells.²¹ Recently, it was shown that silymarin showed estrogenic activity, inhibiting bone loss with mild proliferative effects in the uterus of ovariectomized rats, which was most likely due to a direct interaction of silymarin with estrogen receptors.²⁸ It is deemed that silymarin may be a direct regulator for osteoblast differentiation and bone anabolic formation. In this study, silymarin participated both in the early phase of bone formation and in the late phase of matrix maturation/mineralization.

Matrix mineralization is the accumulation of calcium deposits forming bone nodules, which could be a direct indicator of bone growth.²⁹ Mineralization is accomplished by nucleation of calcium deposits initiated by exocytosis of osteoblast vesicles into the ECM. It was shown that osteoblast vesicles contain ALP, calcium-dependent proteins and calcium-phosphate-phospholipid complexes.³⁰ The vesicles are localized in extracellular clusters with high ALP activity.³¹ Accordingly, the increase (nodule size and abundance) in calcium deposition by silymarin, as microscopically observed alizarin red staining, appeared to be due to elevated cellular ALP levels and matrix vesicle formation. Accordingly, silymarin would stimulate matrix calcium deposits accompanying enhanced uptake of calcium into the matrix vesicles via increased ALP activity. However, the role of silymarin in matrix vesicle-mediated mineralization in osteoblasts remains to be clarified.

Potential mechanism(s) for the enhanced osteogenic activity by silymarin treatment in osteoblasts are not yet defined. It was suggested that silymarin stimulated osteogenic activity via BMP-2-responsive signaling involved in osteoblastic differentiation.¹⁰ BMP initiates signaling by interacting with its distinct serine/threonine kinase receptors that can activate the cytoplasmic SMAD proteins.¹¹ BMP-2 induced expression of Runx2 and osteocalcin.^{5,6} Thus, silymarin-induced up-regulation of bone marker proteins might be a consequence of the elevated induction of BMP-2 by silymarin. As expected, the ALP secretion of MC3T3-E1 osteoblast was abolished by the BMP receptor inhibitor noggin. However, noggin-treated osteoblasts restored ALP secretion back to the basal level. Accordingly, silymarin may boost ALP secretion independent of BMP-2 induction. It was shown that constitutively active SMAD1 induced osteoblastic differentiation of C2C12 myoblasts in cooperation with SMAD4 or Runx2.¹² Similarly, silymarin promoted

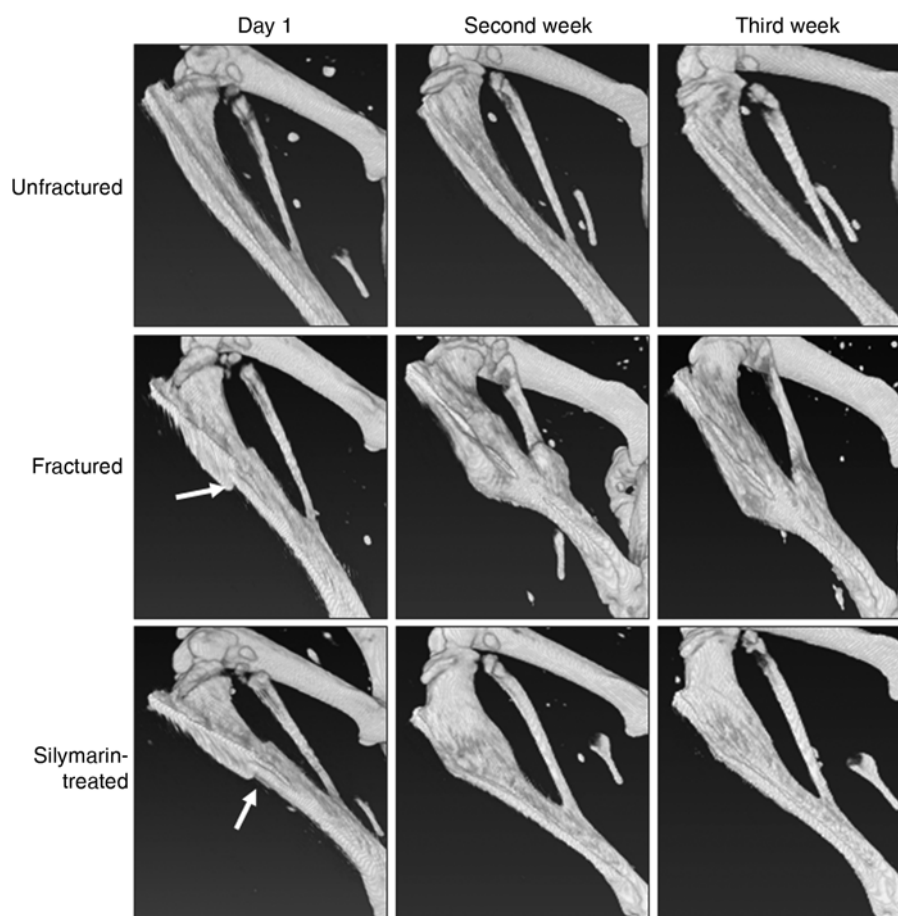


Figure 8 High-resolution three-dimensional radiographic images showing tibial fracture repair of C57BL/6 mice. The animals were divided into three groups. The animals were tibially fractured (fractured) and were orally injected with 10 mg/kg body weight/day silymarin for 21 days (silymarin-treated). Radiographic *in vivo* images for mouse tibial bones were taken on days 1, 7 and 14 after fracture using a MicroCAT II scanner. The arrow indicates the bone fracture site

osteoblastic differentiation through SMAD1/5/8 phosphorylation accompanying nuclear translocation of SMAD4.

Runx2 triggered transcription of collagen type I, osteocalcin, osteopontin and bone sialoprotein via binding its runt homology domain to target promoters and enhancers.⁷ At matrix levels, silymarin accelerated collagen I secretion and calcium deposition for ECM mineralization, most likely due to the increased cellular and matrix activity of ALP, the

major differentiation markers of osteoblasts. Runx2 overexpression in osteoblastic MC3T3-E1 cells increased bone matrix mineralization, indicating that Runx2 plays a stimulatory role in ECM mineralization.^{8,9} This study showed that Runx2 transcription occurred in the early phase of osteoblast proliferation and differentiation. Therefore, it was proposed that silymarin stimulated osteogenic activity by promoting levels of bone marker proteins and enhancing

Table 1 Effects of silymarin treatment on tibial bone density in tibially fractured mice

| Parameters | Mice | Prefracture | Day 1 – postfracture | Day 7 – postfracture | Day 14 – postfracture |
|------------|-------------------|---------------|----------------------|----------------------------|----------------------------|
| BMD | Unfractured | 35.10 ± 1.75 | 41.63 ± 1.72 | 45.96 ± 5.06 | 47.86 ± 2.34 |
| | Fractured | 35.79 ± 1.80 | 41.95 ± 2.40 | 50.84 ± 3.78* | 61.91 ± 2.82* |
| | Silymarin-treated | 34.91 ± 1.84 | 41.26 ± 1.86 | 58.55 ± 2.70* [‡] | 67.36 ± 3.11* [‡] |
| BMC | Unfractured | 7.57 ± 0.56 | 7.25 ± 1.53 | 8.22 ± 2.06 | 8.10 ± 1.21 |
| | Fractured | 7.29 ± 0.64 | 7.82 ± 0.81 | 10.00 ± 1.82* | 12.22 ± 0.79* |
| | Silymarin-treated | 6.98 ± 0.55 | 7.39 ± 1.38 | 11.96 ± 1.89* [‡] | 14.73 ± 0.49* [‡] |
| Area | Unfractured | 0.208 ± 0.008 | 0.211 ± 0.012 | 0.201 ± 0.010 | 0.198 ± 0.011 |
| | Fractured | 0.203 ± 0.008 | 0.208 ± 0.009 | 0.206 ± 0.015 | 0.206 ± 0.009 |
| | Silymarin-treated | 0.199 ± 0.016 | 0.199 ± 0.017 | 0.200 ± 0.014 | 0.198 ± 0.013 |

BMC, bone mineral content; BMD, bone mineral density

Mice were tibially fractured and thereafter orally supplemented with 10 mg/kg body weight/day silymarin for two weeks. All mice received surgical implants in tibiae. Areal BMD (mg/cm²), BMC (mg) and bone width (cm²) were measured in tibial bone by using a PIXImus mouse densitometer. Values are presented as mean ± SEM of six mice

**P* < 0.05, relative to unfractured controls in same column

[‡]*P* < 0.05, relative to fractured mice in same column

Table 2 Effects of silymarin treatment on serum levels of alkaline phosphatase and osteocalcin during 14-day fracture repair periods

| Parameters | Mice | Prefracture | Day 1 – postfracture | Day 7 – postfracture | Day 14 – postfracture |
|-------------|-------------------|-------------|-------------------------|-------------------------|---------------------------|
| ALP | Unfractured | 31.2 ± 2.4 | 19.7 ± 0.9 | 20.0 ± 1.8 | 22.8 ± 2.8 |
| | Fractured | 31.1 ± 2.2 | 19.0 ± 1.3 | 20.2 ± 1.3 | 23.2 ± 1.6 |
| | Silymarin treated | 30.3 ± 2.5 | 19.9 ± 1.0 | 23.4 ± 3.3 | 31.5 ± 4.2 ^{*,‡} |
| Osteocalcin | Unfractured | 31.4 ± 5.4 | 35.1 ± 1.6 | 28.7 ± 5.2 | 28.2 ± 1.7 |
| | Fractured | 34.6 ± 5.8 | 36.1 ± 4.0 | 33.5 ± 4.1 | 31.2 ± 3.0 |
| | Silymarin treated | 33.5 ± 4.8 | 41.8 ± 6.9 [*] | 36.9 ± 5.4 [*] | 38.9 ± 4.7 ^{*,‡} |

Mice were tibially fractured and thereafter orally supplemented with 10 mg/kg body weight/day silymarin for two weeks. All mice received surgical implants in tibiae. Serum alkaline phosphatase (U/L) was measured using the *p*-nitrophenyl phosphate as the substrate. A unit (U) of ALP was defined as release of 1 μ mol *p*-nitrophenol/min. Serum osteocalcin (ng/L) was measured by using enzyme-linked immunosorbent assay kits

ALP, alkaline phosphatase

^{*}*P* < 0.05, relative to unfractured controls in same column

[‡]*P* < 0.05, relative to fractured mice in same column

ECM calcium deposition for matrix mineralization via Runx2-associated pathway(s).

There is so far no ideal drug treatment available to manage osteoporosis leading to fracture. This study attempted to confirm the osteogenic activity of silymarin in the mouse fracture model. The use of the murine fracture models may allow study of fracture healing and bone regeneration.³² The healing sequence of the mouse tibial fracture was similar to that seen in the rat tibia.²⁵ Administration of silymarin was shown to better fracture healing with enhanced bone callus formation during the healing period of 21 days. Serum levels of mesenchymal progenitors of ALP and osteocalcin, indicating osteogenic differentiation, were highly elevated by silymarin after 14-day fracture episodes, compared with fractured mice. Therefore, silymarin appears to play a crucial role in regulating osteogenesis in the later stages and thus may be beneficial for fracture healing. There are limitations in this study by virtue of the small numbers of animals that may create a low power of analysis. Although silymarin had been used in animal fracture experiments, we cannot be sure that the same effects occur in humans. Silymarin affects biological signals of bone tissues via release of anabolic or cytokine molecules. Accordingly, the effects of silymarin may be linked to, or are associated with, the changes in other molecular markers such as vascular endothelial growth factor, extracellular signal-regulated kinase and p38 kinase in the process of fracture healing.^{21,33} Interventions using gene-targeted animals would be necessary for the study of molecular mechanisms of fracture healing and bone regeneration.

In summary, this study showed that silymarin accelerated ALP expression and osteocalcin transcription in MC3T3-E1 cells. At matrix levels, silymarin promoted collagen I secretion and calcium deposition for ECM mineralization, most likely due to the increased ALP activity. Therefore, silymarin can invigorate bone-forming activity directly through triggering BMP-2- and Runx2-targeted osteoblast differentiation and bone marker gene expression. In the mouse fracture healing model, silymarin supplementation improved tibial healing with elevated BMD and serum levels of ALP and osteocalcin. These results demonstrate for the first time that silymarin has a potential to enhance osteoblastogenesis likely via the BMP/SMAD/Runx2 signal pathways and to improve fracture healing and bone

strength in mouse tibiae. Further studies will be necessary to clarify the molecular mechanisms underlying the fracture healing activity of silymarin.

Author contributions: All authors participated in the design, interpretation of the studies and analysis of the data and review of the manuscript. J-LK and S-HP conducted the experiments; DJ and J-SN analyzed animal data; and J-LK and Y-HK wrote the manuscript.

ACKNOWLEDGEMENTS

This study was supported by a grant from the Ministry of Knowledge Economy through Technological Development Project for Regional Industry (70008048), and by a Korea Research Foundation grant funded by the Korean Government (MEST), the Regional Research Universities Program/Medical and Bio-Materials Research Center.

REFERENCES

- Henriksen K, Neutsky-Wulff AV, Bonewald LF, Karsdal MA. Local communication on and within bone controls bone remodeling. *Bone* 2009;**44**:1026–33
- Gaur T, Hussain S, Mudhasani R, Parulkar I, Colby JL, Frederick D, Kream BE, van Wijnen AJ, Stein JL, Stein GS, Jones SN, Lian JB. Dicer inactivation in osteoprogenitor cells compromises fetal survival and bone formation, while excision in differentiated osteoblasts increases bone mass in the adult mouse. *Dev Biol* 2010;**340**:10–21
- Hu ZM, Peel SA, Ho SK, Sandor GK, Clokie CM. Induction of bone matrix protein expression by native bone matrix proteins in C2C12 culture. *Biomed Environ Sci* 2009;**22**:164–9
- Kwon IS, Cho YE, Lomeda RA, Shin HI, Choi JY, Kang YH, Beattie JH. Zinc deficiency suppresses matrix mineralization and retards osteogenesis transiently with catch-up possibly through Runx 2 modulation. *Bone* 2010;**46**:732–41
- Komori T. Regulation of bone development and maintenance by Runx2. *Front Biosci* 2008;**13**:898–903
- Huang W, Yang S, Shao J, Li YP. Signaling and transcriptional regulation in osteoblast commitment and differentiation. *Front Biosci* 2007;**12**:3068–92
- Franceschi RT, Ge C, Xiao G, Roca H, Jiang D. Transcriptional regulation of osteoblasts. *Ann NY Acad Sci* 2007;**1116**:196–207
- Kaji H, Naito J, Sowa H, Sugimoto T, Chihara K. Smad3 differently affects osteoblast differentiation depending upon its differentiation stage. *Horm Metab Res* 2006;**38**:740–5
- Hinoi E, Fujimori S, Wang L, Hojo H, Uno K, Yoneda Y. Nrf2 negatively regulates osteoblast differentiation via interfering with Runx2-dependent transcriptional activation. *J Biol Chem* 2006;**281**:18015–24

- 10 Chen D, Zhao M, Mundy GR. Bone morphogenetic proteins. *Growth Factors* 2004;**22**:233–41
- 11 Li B. Bone morphogenetic protein-Smad pathway as drug targets for osteoporosis and cancer therapy. *Endocr Metab Immune Disord Drug Targets* 2008;**8**:208–19
- 12 Lo YC, Chang YH, Wei BL, Huang YL, Chiou WF. Betulinic acid stimulates the differentiation and mineralization of osteoblastic MC3T3-E1 cells: involvement of BMP/Runx2 and beta-catenin signals. *J Agric Food Chem* 2010;**58**:6643–9
- 13 Shapiro F. Bone development and its relation to fracture repair. The role of mesenchymal osteoblasts and surface osteoblasts. *Eur Cell Mater* 2008;**15**:53–76
- 14 Schindeler A, McDonald MM, Bokko P, Little DG. Bone remodeling during fracture repair: the cellular picture. *Semin Cell Dev Biol* 2008;**19**:459–66
- 15 Parfitt AM. Trabecular bone architecture in the pathogenesis and prevention of fracture. *Am J Med* 1987;**82**:68–72
- 16 Lee DY, Liu Y. Molecular structure and stereochemistry of silybin A, silybin B, isosilybin A, and isosilybin B, isolated from *Silybum marianum* (milk thistle). *J Nat Prod* 2003;**66**:1171–4
- 17 Muriel P. NF- κ B in liver diseases: a target for drug therapy. *J Appl Toxicol* 2009;**29**:91–100
- 18 Ziolkowska A, Rucinski M, Pucher A, Tortorella C, Nussdorfer GG, Malendowicz LK. Expression of osteoblast marker genes in rat calvarial osteoblast-like cells, and effects of the endocrine disruptors diphenylolpropane, benzophenone-3, resveratrol and silymarin. *Chem Biol Interact* 2006;**164**:147–56
- 19 Reinwald S, Weaver CM. Soy isoflavones and bone health: a double-edged sword? *J Nat Prod* 2006;**69**:450–9
- 20 Trzeciakiewicz A, Habauzit V, Mercier S, Lebecque P, Davicco MJ, Coxam V, Demigne C, Horcajada MN. Hesperetin stimulates differentiation of primary rat osteoblasts involving the BMP signalling pathway. *J Nutr Biochem* 2010;**21**:424–31
- 21 Kuo PL, Hsu YL, Chang CH, Chang JK. Osteole-mediated cell differentiation through bone morphogenetic protein-2/p38 and extracellular signal-regulated kinase 1/2 pathway in human osteoblast cells. *J Pharmacol Exp Ther* 2005;**314**:1290–9
- 22 Kang SW, Choi JS, Bae JY, Li J, Kim DS, Kim JL, Shin SY, You HJ, Park H, Ji GE, Kang YH. Blockade of vascular angiogenesis by *Aspergillus usamii* var. *shirousamii*-transformed *Angelicae gigantis* Radix and *Zizyphus jujube*. *Nutr Res Pract* 2009;**3**:3–8
- 23 Akcakaya H, Aroymak A, Gokce SA. Quantitative colorimetric method of measuring alkaline phosphatase activity in eukaryotic cell membranes. *Cell Biol Int* 2007;**31**:186–90
- 24 Hale LV, Ma YF, Santerre RF. Semi-quantitative fluorescence analysis of calcein binding as a measurement of *in vitro* mineralization. *Calcif Tissue Int* 2000;**67**:80–4
- 25 Bonnrens F, Einhorn A. Production of a standard closed fracture in laboratory animal bone. *J Orthop Res* 1984;**2**:97–101
- 26 Hiltunen A, Vuorio E, Aro HT. A standardized experimental fracture in the mouse tibia. *J Orthop Res* 1993;**11**:305–12
- 27 Komori T. Regulation of osteoblast differentiation by transcription factors. *J Cell Biochem* 2006;**99**:1233–9
- 28 El-Shitany NA, Hegazy S, El-Desoky K. Evidences for antiosteoporotic and selective estrogen receptor modulator activity of silymarin compared with ethinylestradiol in ovariectomized rats. *Phytomedicine* 2010;**17**:116–25
- 29 Kirsch T, Harrison G, Worch KP, Golub EE. Regulatory roles of zinc in matrix vesicle mediated mineralization of growth plate cartilage. *J Bone Min Res* 2000;**15**:261–70
- 30 Anderson HC. Molecular biology of matrix vesicles. *Clin Orthop Relat Res* 1995;**314**:266–80
- 31 Kanno S, Anuradha CD, Hirano S. Localization of zinc after *in vitro* mineralization in osteoblastic cells. *Biol Trace Elem Res* 2001;**83**:39–47
- 32 Holstein JH, Garcia P, Histing T, Kristen A, Scheuer C, Menger MD, Pohlemann T. Advances in the establishment of defined mouse models for the study of fracture healing and bone regeneration. *J Orthop Trauma* 2009;**23**:S31–8
- 33 Huh JE, Kwon NH, Baek YH, Lee JD, Choi DY, Jingushi S, Kim KI, Park DS. Formononetin promotes early fracture healing through stimulating angiogenesis by up-regulating VEGFR-2/Flk-1 in a rat fracture model. *Int Immunopharmacol* 2009;**9**:1357–65

(Received November 7, 2011, Accepted December 28, 2011)